Nonlinear elasticity of stiff biopolymers connected by flexible linkers

K. E. Kasza,[1] G. H. Koenderink,[1,*] Y. C. Lin,[1] C. P. Broedersz,[3] W. Messner,[2,†] F. Nakamura,[2] T. P. Stossel,[2] F. C. MacKintosh,[3] and D. A. Weitz[1]

[1]*Department of Physics and SEAS, Harvard University, Cambridge, Massachusetts 02138, USA*

[2]*Department of Medicine, Translational Medicine Division, Brigham and Women's Hospital, Harvard Medical School, Boston, Massachusetts 02115, USA*

[3]*Department of Physics and Astronomy, Vrije Universiteit, 1081 HV Amsterdam, The Netherlands*

(Received 27 September 2007; revised manuscript received 13 February 2009; published 29 April 2009)

Networks of the biopolymer actin, cross-linked by the compliant protein filamin, form soft gels. They can, however, withstand large shear stresses due to their pronounced nonlinear elastic behavior. The nonlinear elasticity can be controlled by varying the number of cross-links per actin filament. We propose and test a model of rigid filaments decorated by multiple flexible linkers that is in quantitative agreement with experiment. This allows us to estimate loads on individual cross-links, which we find to be less than 10 pN.

DOI: 10.1103/PhysRevE.79.041928 PACS number(s): 87.16.Ka, 83.60.Df, 87.15.La

Cells interact mechanically with their environment largely through their *cytoskeleton*, a mechanical framework consisting of filamentous protein polymers and associated proteins that regulate cytoskeletal microstructure and connectivity [1,2]. The *in vivo* cytoskeleton is remarkably complex, making *in vitro* studies of purified cytoskeletal networks useful for elucidating basic physical principles governing cytoskeletal mechanics [3,4] and mechanosensing [5]. Networks of filamentous actin (*F*-actin), a major component of the cytoskeleton, exhibit unusual material properties [6–14]. Among the most striking properties is a strongly nonlinear response to shear [6–10]; this depends sensitively on the cross-linking protein. For noncompliant cross-links, the network response arises from the compliance of the actin filaments themselves [7–10,15]. By contrast, for compliant cross-links, such as those commonly found in cells, actin networks exhibit dramatically different elasticity [16–19]. One such cross-link is human filamin, a large protein with a contour length of 150 nm [20,21], [Fig. 1(b)]. For small forces, filamin behaves like a flexible wormlike chain; whereas for forces larger than 50–100 pN, unfolding of individual Ig-like domains occurs [22]. Human filamin forms a weak gel with *F*-actin, with linear shear moduli of ~1 Pa. However, these gels exhibit a large mechanical stiffening under strain [16,17], and can withstand very large stresses, as high as 100 Pa, at shear strains of order of one. A theoretical understanding of the molecular origins of this unusual behavior will help elucidate the basic design principles of cytoskeletal mechanics.

Here, we show that the nonlinear elastic behavior of filamin-*F*-actin gels is controlled by the number of cross-links per actin filament, and we account for this unusual behavior by modeling the networks as rigid rods connected with multiple flexible linkers [23]. The model quantitatively explains the dramatic nonlinear stiffening of filamin-*F*-actin networks, providing fundamental insight into its origins. It also provides an estimate of the maximum load experienced by individual cross-links, which is less than 10 pN, too small to result in significant unfolding of filamin Ig-like domains.

We reconstitute networks of *F*-actin cross-linked with filamin *A* using purified monomeric actin, filamin *A* [24], and gelsolin [25]. We control network microstructure by varying the actin concentration, c_A, and the molar ratio of filamin dimers to actin monomers, $R_{F/A}$. In addition, we regulate the actin filament length distribution by adding the capping protein gelsolin. The molar ratio of gelsolin to actin monomers, $R_{G/A}$, sets the mean actin filament length, which is approxi-

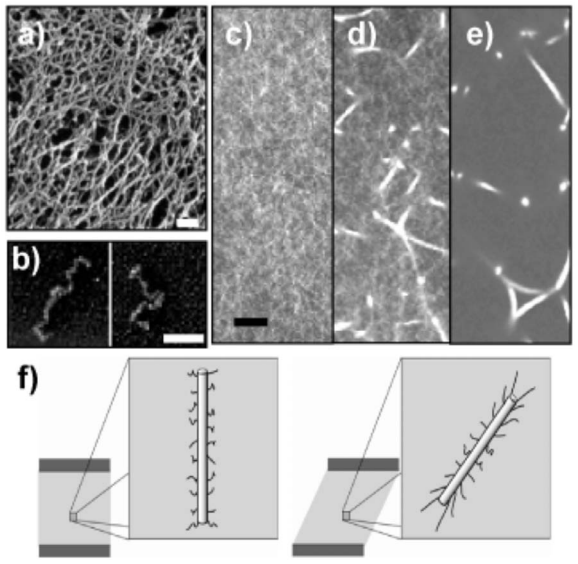

FIG. 1. (a) Electron micrograph of a fixed and rotary-shadowed filamin-*F*-actin network at $c_A=1$ mg/ml, $L=15$ μm, and $R_{F/A}=0.005$. Scale bar=100 nm. (b) Electron micrograph of rotary-shadowed filamin molecules. Scale bar=50 nm. [(c)–(e)] Confocal images of various networks. Scale bar=5 μm. $c_A=0.5$ mg/ml with $L=15$ μm and (c) $R_{F/A}=0.002$ or (d) $R_{F/A}=0.01$, or (e) $L=1$ μm and $R_{F/A}=0.04$. (f) Schematic of proposed actin-filamin elastic element with $n=20$, embedded in an unsheared (left) and sheared (right) network.

*Present address: AMOLF Institute, Amsterdam, The Netherlands.

†Present address: Department of Mechanical Engineering, Carnegie Mellon University, Pittsburgh, PA 15213, USA.

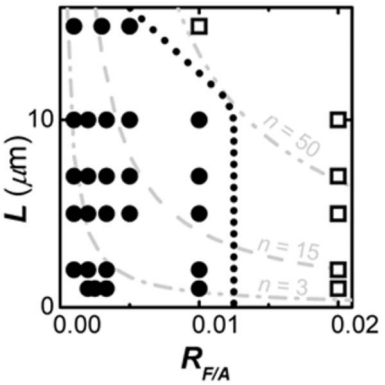

FIG. 2. Parameter space of network microstructure for an actin concentration of 0.5 mg/ml with molar ratios, $R_{F/A}$, and mean actin filament lengths, L. Nonbundled (closed circles) and bundled (open squares) networks, as determined by confocal microscopy. Dotted line denotes transition in network microstructure from nonbundled to bundled F-actin. Dashed lines represent constant number of filamins per actin filament, n.

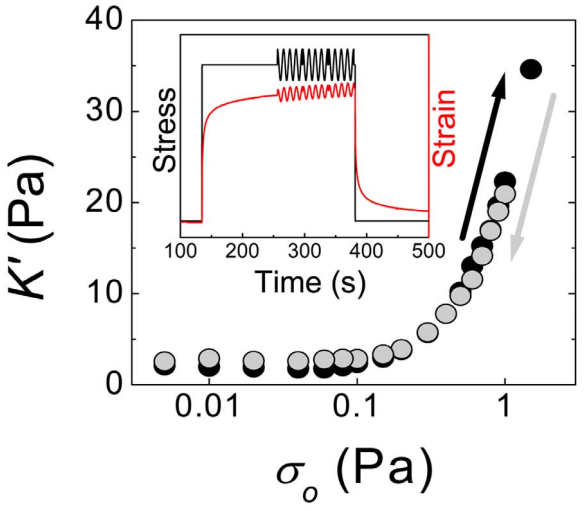

FIG. 3. (Color online) To measure the nonlinear differential elastic response at a particular prestress, σ_o, a small, oscillatory stress is superposed on a static stress σ_o and the resulting oscillatory strain is measured (inset). For a typical actin-filamin network with c_A=0.5 mg/ml, $R_{F/A}$=0.005, and L=15 μm, σ_o can be increased to just below the maximum stress supported by the network and decreased again with minimal hysteresis in the differential elastic modulus, $K'(\sigma_o)$.

mately $L=(370\ R_{G/A})^{-1}$ μm [26,27]. Samples are prepared by mixing solutions of 10x polymerization buffer (20 mM Tris-HCl, 20 mM $MgCl_2$, 1 M KCl, 2 mM DTT, 2 mM $CaCl_2$, 5 mM ATP, pH 7.5), gelsolin, filamin, and monomeric actin. After mixing, the sample is loaded into a microscope chamber, consisting of two cover slips with a 1 mm spacer, or between the plates of a rheometer. It is allowed to polymerize for 1 h at 25 °C. Fluorescently labeled networks for imaging are polymerized in the presence of 0.6 μM Alexa-488 phalloidin.

We use a confocal microscope to image microstructure. At c_A=0.5 mg/ml and low cross-link density, the network is a fine homogeneous mesh of F-actin and nearly indistinguishable in appearance from entangled F-actin, as shown in Fig. 1(c). Electron micrographs confirm the networks are an isotropic homogeneous mesh that mimics the actin cortex of cells [Fig. 1(a)]. Above a threshold value of $R_{F/A}\approx 0.01$, for c_A=0.5 mg/ml, large actin bundles appear [Fig. 1(d)]; with increasing $R_{F/A}$, more actin partitions into the bundles [Figs. 1(c)–1(e)]. The bundling transition depends on c_A but only weakly on L (Fig. 2).

To investigate the elastic response of the filamin-F-actin networks, we use a stress-controlled rheometer with 40 mm parallel plates and an 80 μm gap. We confirm that the results are independent of gap and use a solvent trap to minimize evaporation. To precisely measure the nonlinear elasticity, we use a differential measurement [7,16]: we superpose a small oscillatory stress, $\delta\sigma(\omega)$, on a static "prestress," σ_o, and measure the resulting oscillatory strain, $\delta\gamma(\omega)$ (inset of Fig. 3) We determine the differential modulus, $K^*(\sigma_o,\omega)=[\delta\sigma(\omega)/\delta\gamma(\omega)]|_{\sigma_o}$, at 0.6 rad/s and ensure linear response by maintaining $\delta\gamma<2\%$. We confirm that, at each level of prestress, K^* shows no time dependence and that there is minimal hysteresis in $K^*(\sigma_o)$ as shown in Fig. 3

For a network with short F-actin filaments, having c_A =0.5 mg/ml, L=1 μm, and $R_{F/A}$=0.003, the differential elastic modulus, K', is 0.3 Pa and is nearly independent of prestress before network breakage at a maximum stress, σ_m, of 0.4 Pa [black squares, inset of Fig. 4(a)]. Increasing L fivefold yields a network with nearly identical linear modulus; however, it stiffens for prestresses above a critical prestress, σ_c=0.2 Pa [black triangles, inset of Fig. 4(a)]. While $\sigma_o<\sigma_c$, the response is linear and K' is identical to the linear elastic modulus, G_0. The network eventually breaks at σ_m =0.6 Pa, having reached a maximum differential modulus, K'_m, of 1.6 Pa. As we increase L further, σ_m and K'_m continue to increase [black circles, inset of Fig. 4(a)]. This L-dependent stiffening provides an alternate control parameter for tuning nonlinear elasticity in filamin-F-actin networks, in addition to $R_{F/A}$ [16].

The nonbundled filamin-F-actin networks can stiffen to K'=100 Pa and support stresses up to nearly 10 Pa before breaking [inset of Fig. 4(a)]. Networks with bundles show qualitatively similar nonlinear behavior but can stiffen to $K'>2000$ Pa and support stresses of more than 80 Pa [inset of Fig. 4(b)]. In contrast to other bundled actin networks [28], the bundled filamin-F-actin gels are soft with G_0 <10 Pa regardless of c_A or $R_{F/A}$ while the amount of stiffening increases with $R_{F/A}$ (Figs. 4 and 5).

To quantify the variations in the nonlinear elastic response, we investigate the dependence on the control parameters $R_{F/A}$, $R_{G/A}$, and c_A. For c_A=0.5 mg/ml (black) and L =15 μm (circles) with sparse cross-linking ($R_{F/A}$=0.0003), σ_m is threefold larger than for purely entangled actin [Fig. 5(a)]. The maximum stress is independent of $R_{F/A}$ up to 0.001, as shown by the $R_{F/A}$ dependence in Fig. 5(a). Upon increasing $R_{F/A}$ further, σ_m increases nearly linearly with $R_{F/A}$, up to a maximum of 5 Pa before the networks become bundled. Once bundles appear, σ_m continues to increase with $R_{F/A}$ [open symbols, Fig. 5(a)]. For L=7 μm (inverted triangles), σ_m for all $R_{F/A}$ is smaller than for the longer fila-

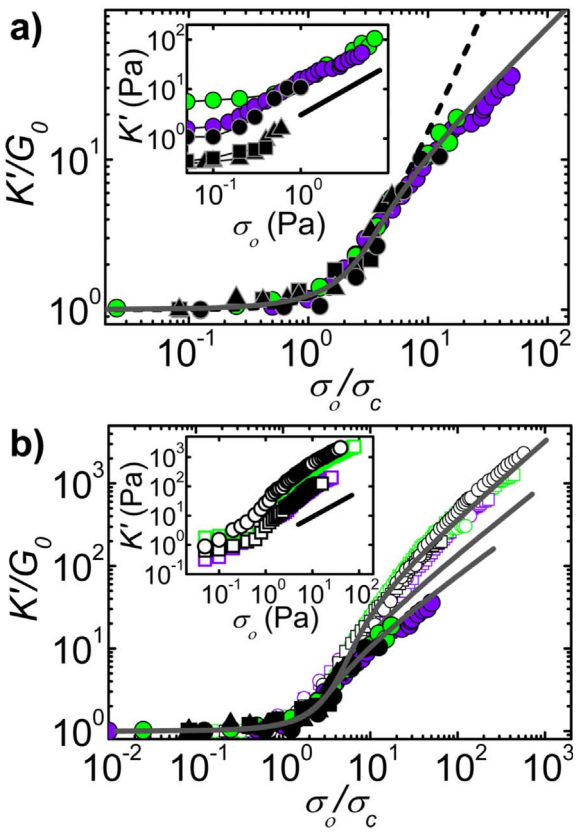

FIG. 4. (Color online) [(a) and (b)] Nonlinear elastic response of filamin-*F*-actin networks. c_A=0.5 (black), 1.0 (dark gray, purple online), and 1.5 mg/ml (light gray, green online). L=1 μm (squares), L=5 μm (triangles), and L=15 μm (circles). (a) Rescaled $K'/G_0(\sigma_o/\sigma_c)$ for nonbundled networks. Prediction by self-consistent effective-medium model of stiff filaments connected by multiple flexible linkers (solid line). Prediction for a network of semiflexible filaments connected by rigid pointlike linkers, $K' \sim \sigma_o^{3/2}$ (dashed line) [7]. Inset: representative $K'(\sigma_o)$ for nonbundled networks. $R_{F/A}$=0.003 for all except the light gray (green online) circles having $R_{F/A}$=0.002. Line indicates linear scaling. (b) Comparison of rescaled nonlinear elastic response of nonbundled (closed symbols) and bundled (open symbols) networks. Predictions of the model in Ref. [23] for three different values of network connectivity (solid lines, with increasing K' for higher connectivity). Inset: $K'(\sigma_o)$ for bundled networks with $R_{F/A}$=0.01. Line indicates linear scaling.

ments. For L=1 μm (squares), σ_m is 0.3 Pa and independent of $R_{F/A}$ up to 0.01 before the network becomes bundled. Increasing c_A to 1.0 mg/ml (dark gray, purple online) and further to 1.5 mg/ml (light gray, green online) at fixed $R_{F/A}$ and L increases σ_m.

In all cases, increasing L shifts the σ_m curve so that the strong dependence on cross-linking begins at smaller $R_{F/A}$. Similar behavior is observed for K'_m [Fig. 5(b)]. Taken together, these data suggest that the structural parameter controlling the nonlinear elastic response is proportional to *both* $R_{F/A}$ and L. This is in contrast to predictions for semiflexible filaments connected by rigid cross-links, where the nonlinear elastic behavior is independent of L [7,15]. To account for this behavior, we hypothesize that the key control parameter

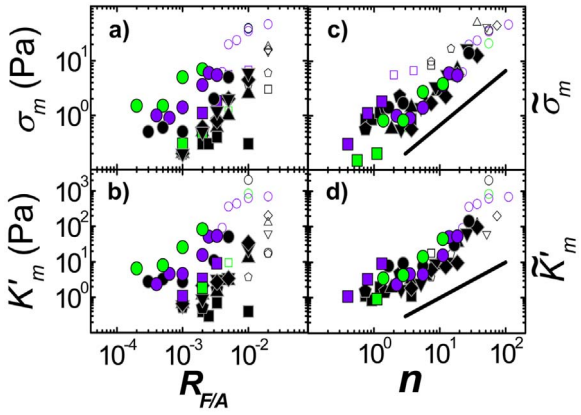

FIG. 5. (Color online) (a) Maximum stress, σ_m, and (b) maximum differential modulus, K'_m, vs $R_{F/A}$. (c) Scaled maximum stress, $\tilde{\sigma}_m=\sigma_m/c_A^{3/2}$, and (d) maximum differential modulus, $\tilde{K}'_m=K'_m/c_A^{3/2}$, vs n. c_A=0.5 mg/ml (black), c_A=1.0 mg/ml (dark gray, purple online), and c_A=1.5 mg/ml (light gray, green online). L=1 μm (squares), L=2 μm (pentagons), L=5 μm (triangles), L=7 μm (inverted triangles), L=10 μm (diamonds), and L=15 μm (circles). Lines denote linear scaling with n.

is the number of filamin dimers per actin filament, $n=R_{F/A}R_{G/A}^{-1}=370R_{F/A}L$; this has the correct scaling and is a measure of network connectivity and hence elasticity.

To test this hypothesis, we propose a model that directly incorporates the flexible nature of the filamin molecule, and allows the cross-link compliance to dominate the network compliance [23]. We first focus on low cross-linking densities in the absence of bundles. The basic elastic element is a rigid actin filament of length L decorated with n flexible linkers, as depicted in Fig. 1(f). Each linker is a soft linear spring that becomes rigid upon being stretched to a maximum extension, l_o, and detaches from the rigid rod at a maximum force, f_m. A network of these elastic elements that deforms affinely under shear will have a linear response only so long as every linker has extension less than l_o. The stress is then a sum of forces on the individual filaments per unit area in the network: $\sigma \approx \langle\tau\rangle/\xi^2$, where $\langle\tau\rangle$ is the average tension along the actin filament and $\xi \sim c_A^{-1/2}$ is the mesh size. A naïve estimate of the maximum tension at network failure would be $\langle\tau\rangle \approx nf_m$, which results in $\sigma_m \sim nc_A$. However, this does not account for the three-body nature of filamin-*F*-actin cross-linking: the probability to form an effective cross-link requires binding to *two* actin filaments. This adds a factor of $\xi^{-1} \sim c_A^{1/2}$, which measures the linear density of neighboring actin filaments along a particular filament. The scaling prediction then becomes $\sigma_m \sim nc_A^{3/2}$.

To test this prediction, we scale σ_m from Fig. 5(a) by $c_A^{3/2}$, $\tilde{\sigma}_m=\sigma_m/c_A^{3/2}$. When plotted as a function of n, the data for the nonbundled networks do indeed collapse onto a single curve, as shown by the closed symbols in Fig. 5(c). For $n \gtrsim 3$, $\tilde{\sigma}_m$ has a nearly linear dependence on n, in agreement with the prediction of the model. The somewhat stronger than linear scaling with n may indicate additional cooperativity beyond our simple model. For $n \lesssim 3$, the networks are weakly connected and support only very small shear stresses, nearly independent of n. The scaled data for the bundled networks

also collapse but onto a separate curve, which has a larger magnitude and somewhat weaker n dependence than the nonbundled networks [open symbols, Fig. 5(c)]. A similar collapse is observed for $\tilde{K}'_m = K'_m / c_A^{3/2}$, when it is plotted as a function of n, as shown in Fig. 5(d). These results confirm our hypothesis that n is a key control parameter for the network mechanics.

The approximately linear dependence of σ_m on n in Fig. 5 suggests that network failure corresponds to a particular force per filamin cross-link. This failure is likely due to filamin unbinding from actin. From the schematic in Fig. 1(f), the maximum tension in a typical actin filament occurs at its midpoint, and is given by the sum of forces applied by the filamins bound on each side of the midpoint. For large n, these forces should increase linearly away from this midpoint, which leads to $\langle \tau \rangle = n f_0 / 6$, where f_0 is the *maximum* force experienced by a filamin. For an isotropic network, the shear stress is given by $\sigma = \frac{2}{15} \rho \langle \tau \rangle_m$, where $\rho \sim \xi^{-2}$ is the density of polymer length per volume and $\langle \tau \rangle_m$ refers to the average tension along actin filaments oriented in the direction of maximal network extension. These are the filaments expected to be under the greatest tension. For a 1 mg/ml network, $\rho \approx 40\ \mu\text{m}^{-2}$, which sets $\langle \tau \rangle_m \approx 2$ pN for $\sigma_m = 10$ Pa. This force is the result of multiple filamins n, as noted above. Thus, the load on any individual filamin is less than 2 pN at network failure under the conditions of our experiments, corresponding to loading rates of 0.1–1 pN/s. This is comparable to rupture forces measured for a number of actin binding proteins [15,29–31] but is far below the 50–100 pN forces required for full unfolding of individual Ig domains in filamin [22]. Indeed, recent single molecule studies indicate that filamin unbinding is favored over unfolding at loading rates below 50 pN/s [31]. Thus, we believe that network failure is a result of filamin unbinding and that filamin Ig domain unfolding is unlikely [19].

If we scale K' by G_0 and σ_o by σ_c, data from all the nonbundled networks collapse onto a single curve [Fig. 4(a)]. Interestingly, K' for these networks does not increase as a well-defined power law in σ_o having a stronger than linear dependence for small σ_o before becoming nearly linear at large σ_o [Fig. 4(a)]. These observations are in contrast with those for actin cross-linked with the noncompliant protein scruin, for which K' is predicted and observed to increase as $\sigma_o^{3/2}$ [7,9], [dashed line, Fig. 4(a)]. The K' curves from the bundled networks also collapse onto a single rescaled curve, which is distinct from that of the nonbundled networks [Fig. 4(b)]. Compared to the nonbundled networks, the bundled networks show greatly enhanced stiffening but retain the same linear dependence of $K'(\sigma_o)$ at high stress [Fig. 4(b)]. However, the crossover to the nearly linear dependence on σ_o occurs at larger stresses for the bundled networks.

The shape of both these curves is consistent with the predictions of the self-consistent effective-medium model of stiff filaments connected by multiple flexible linkers [23] for different values of network connectivity [solid lines, Figs. 4(a) and 4(b)], which determines the crossover to an asymptotic high-stress regime where the stiffness increases linearly with stress in all cases. The bundled data are consistent with the predictions for higher connectivity. Importantly, this linear dependence is insensitive to the parameters of this model and is consistent not only with our experiments but also with prior reports [16,17]. This is strong evidence that, regardless of detailed network microstructure, the mechanism underlying strain stiffening in filamin-*F*-actin is not governed purely by the nonlinear force-extension curve of actin filaments themselves [7,9] but rather by the flexible cross-links.

The quantitative agreement between our model and our experimental data provides confirmation of our understanding of the underlying principles of the mechanics of *F*-actin networks with highly flexible cross-links. The mechanism underlying these networks' remarkable strength may be exploited for building highly compliant yet strong synthetic materials. The model can be used to estimate the conditions required for forced unfolding of cross-links inside living cells [32]. Moreover, our results will serve as an important step in developing more sophisticated models of cytoskeletal mechanics.

We thank J. Hartwig for EM imaging and C. Storm for helpful discussions. This work was supported by the NSF (Contracts No. DMR-0602684 and No. CTS-0505929), the Harvard MRSEC (Contract No. DMR-0820484), and FOM. K.E.K. was supported by the DoD and the NSF. G.H.K. was supported by a European Marie Curie Grant (Grant No. FP6-2002-Mobility-6B, 8526). W.M. was supported by the National Heart, Lung, and Blood Institute (Grant No. 1 F33 HL083684-01). The confocal microscope was maintained by the Harvard Center for Nanoscale Systems.

[1] T. D. Pollard and J. A. Cooper, Annu. Rev. Biochem. **55**, 987 (1986).
[2] T. P. Stossel *et al.*, Annu. Rev. Cell Biol. **1**, 353 (1985).
[3] B. D. Hoffman *et al.*, Proc. Natl. Acad. Sci. U.S.A. **103**, 10259 (2006).
[4] N. Wang *et al.*, Am. J. Physiol. Cell Physiol. **282**, C606 (2002).
[5] D. E. Discher, P. Janmey, and Y. L. Wang, Science **310**, 1139 (2005).
[6] O. Chaudhuri, S. H. Parekh, and D. A. Fletcher, Nature (London) **445**, 295 (2007).
[7] M. L. Gardel *et al.*, Science **304**, 1301 (2004).
[8] M. L. Gardel *et al.*, Phys. Rev. Lett. **93**, 188102 (2004).
[9] F. C. MacKintosh, J. Kas, and P. A. Janmey, Phys. Rev. Lett. **75**, 4425 (1995).
[10] C. Storm *et al.*, Nature (London) **435**, 191 (2005).
[11] D. A. Head, A. J. Levine, and F. C. MacKintosh, Phys. Rev. Lett. **91**, 108102 (2003).

[12] J. Wilhelm and E. Frey, Phys. Rev. Lett. **91**, 108103 (2003).
[13] P. A. Janmey *et al.*, Nature Mater. **6**, 48 (2007).
[14] J. Liu *et al.*, Phys. Rev. Lett. **98**, 198304 (2007).
[15] R. Tharmann, M. M. Claessens, and A. R. Bausch, Phys. Rev. Lett. **98**, 088103 (2007).
[16] M. L. Gardel *et al.*, Proc. Natl. Acad. Sci. U.S.A. **103**, 1762 (2006).
[17] M. L. Gardel *et al.*, Phys. Rev. Lett. **96**, 088102 (2006).
[18] B. Wagner *et al.*, Proc. Natl. Acad. Sci. U.S.A. **103**, 13974 (2006).
[19] B. A. DiDonna and A. J. Levine, Phys. Rev. Lett. **97**, 068104 (2006).
[20] T. P. Stossel *et al.*, Nat. Rev. Mol. Cell Biol. **2**, 138 (2001).
[21] F. Nakamura *et al.*, J. Cell Biol. **179**, 1011 (2007).
[22] S. Furuike, T. Ito, and M. Yamazaki, FEBS Lett. **498**, 72 (2001).
[23] C. P. Broedersz, C. Storm, and F. C. MacKintosh, Phys. Rev. Lett. **101**, 118103 (2008).
[24] F. Nakamura *et al.*, J. Biol. Chem. **277**, 9148 (2002).
[25] D. J. Kwiatkowski, P. A. Janmey, and H. L. Yin, J. Cell Biol. **108**, 1717 (1989).
[26] P. A. Janmey *et al.*, J. Biol. Chem. **261**, 8357 (1986).
[27] D. Biron and E. Moses, Biophys. J. **86**, 3284 (2004).
[28] O. Lieleg *et al.*, Phys. Rev. Lett. **99**, 088102 (2007).
[29] H. Miyata, R. Yasuda, and K. Kinosita, Jr., Biochim. Biophys. Acta **1290**, 83 (1996).
[30] T. Nishizaka *et al.*, Nature (London) **377**, 251 (1995).
[31] J. M. Ferrer *et al.*, Proc. Natl. Acad. Sci. U.S.A. **105**, 9221 (2008).
[32] C. P. Johnson *et al.*, Science **317**, 663 (2007).